THE JOURNAL OF PHYSICAL CHEMISTRY B

Article

pubs.acs.org/JPCB

Oxidation-Induced Photoluminescence of Conjugated Polymers

Ma. Helen M. Cativo,[†,⊥] Amanda C. Kamps,[†,⊥] Jian Gao,[§] John K. Grey,*[,§] Geoffrey R. Hutchison,*[,‡] and So-Jung Park*[,†]

[†]Department of Chemistry, University of Pennsylvania, 231 South 34th Street, Philadelphia, Pennsylvania 19104, United States

[‡]Department of Chemistry, University of Pittsburgh, 219 Parkman Avenue, Pittsburgh, Pennsylvania 15260, United States

[§]Department of Chemistry, University of New Mexico, MSC03 2060, Albuquerque, New Mexico 87131, United States

Supporting Information

ABSTRACT: Here, we report an unusual oxidation-induced photoluminescence (PL) turn-on response of a poly(3-alkoxythiophene), poly(3-{2-[2-(2-ethoxyethoxy)ethoxy]-ethoxy}thiophene) (PEEEET). PEEEET shows a significantly red-shifted absorption spectrum compared to polyalkylthiophenes and is almost nonfluorescent (quantum yield ≪ 1%) in its pristine state. The introduction of sulfonyl defects along the polymer backbone by the oxidation of PEEEET with *meta*-chloroperbenzoic acid (*m*-CPBA) increased the emission quantum yield with the intensity increasing with the degree of oxidation. Molecular modeling data indicated that the oxidation-induced PL increase cannot be explained by the nature of monomer units and radiative rate changes. We attributed the enhanced fluorescence to the reduced nonradiative rate caused by the increased band gap, according to the energy gap law, which is consistent with the observed blue shifts in absorption and PL spectra accompanied by the PL increase.

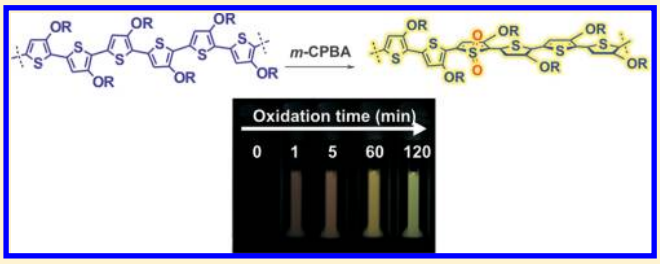

1. INTRODUCTION

Conjugated polymers are an important class of materials that has resulted in a number of innovations in modern science and technology. Owing to their unique optical and transport properties and solution processability, conjugated polymers have been widely utilized in various applications ranging from light-emitting diodes (LED)[1] and photovoltaics[2] to biological sensing[3−5] and imaging.[6−8] The organic semiconductors are, however, prone to oxidation when they are exposed to air and light; in fact, this oxidative damage has been the main hurdle in many applications of conjugated polymers mentioned above. Photooxidation is more problematic for light-based applications such as LED and fluorescence-based imaging because the oxidation products typically act as efficient luminescence quenchers. In polyphenylenevinylenes, for example, it was suggested that the reaction between the polymer and singlet oxygen generates carboxyl defects that act as efficient photoluminescence (PL) quenchers.[9] In other studies, the oxidation-induced reversible PL quenching of poly[2-methoxy-5-(2′-ethylhexyloxy)-*p*-phenylenevinylene] (MEH-PPV) was attributed to hole polarons generated from photooxidation.[10] In poly(3-alkylthiophenes), singlet oxygen was reported to be responsible for polymer degradation and photobleaching in solution,[11,12] while other studies suggested free radical pathways as the main oxidative degradation mechanisms of thin films.[13,14] Although the mechanisms are not yet fully understood, oxidation-induced PL quenching is a common phenomena among most conjugated polymers,[1,15] and thus, developing oxidation-resistant polymers has been an important research topic in this area.[16]

On the other hand, there are some rare examples of conjugated polymers that show increased PL quantum yield upon oxidation. A few epoxide defects in MEH-PPV were shown to increase the PL quantum yield (QY), although the brightness of oxidized polymers remained close to that of pristine polymers due to the reduction in the absorption coefficient.[17] Swager and co-workers showed that the oxidation of thioether side chains of poly(*p*-phenyleneethynylene) switched the polymer from a dark to an emissive polymer.[18] The oxidation-induced PL increase was explained by the increase in the radiative rate due to better molecular orbital overlap. Here, we report a new type of PL turn-on response of a conjugated polymer, poly(3-{2-[2-(2-ethoxyethoxy)ethoxy]-ethoxy}thiophene) (PEEEET) (Figure 1). In its pristine state, PEEEET is almost nonemissive and has a very low QY (≪1%) like other polyalkoxythiophenes.[19−22] Upon exposure to an oxidant such as *meta*-chloroperbenzoic acid (*m*-CPBA), PEEEET becomes emissive under UV irradiation. We attribute this unusual phenomenon to the reduced nonradiative rate, a different mechanism from the report[18] by the Swager group mentioned above. On the basis of spectroscopic measurements and molecular modeling, the oxidation-induced PL turn-on of PEEEET is attributed to the reduction of a nonradiative rate induced by the band gap increase and the distortion of the

Special Issue: Paul F. Barbara Memorial Issue

Received: August 30, 2012
Revised: November 16, 2012
Published: November 28, 2012

 © 2012 American Chemical Society

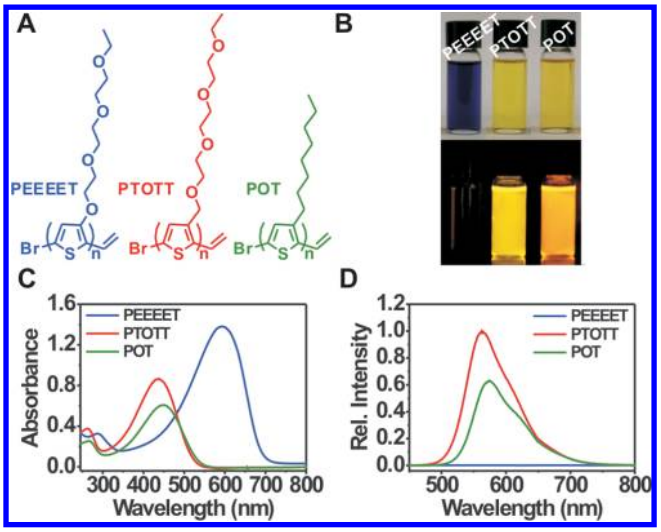

Figure 1. (A) Chemical structures of the three polymers used in this study. (B) Photograph of the polymer solutions under ambient light (top) and under UV irradiation (bottom) (λ_{exc} = 365 nm). (C) Electronic absorption spectra and (D) PL spectra of the polymers in chloroform (5.14 μM, λ_{exc} = 430 nm).

planar conformation of pristine PEEEET upon oxidation. We believe that this is the first report that describes a PL turn-on response upon the direct oxidation of the conjugated backbone.

2. MATERIALS AND METHODS

2.1. Materials. Chloroform, sodium thiosulfate, sodium carbonate, and sodium sulfate were purchased from Fisher Scientific. Coumarin 6 was purchased from Acros Organics. *m*-CPBA (77%), coumarin 102, cresyl violet, rhodamine 6G, and all other reagents were purchased from Aldrich. The exact purity of the active oxidant in the commercial *m*-CPBA/*meta*-chlorobenzoic acid mixture was determined to be 74% by mass using iodometric titration, following the typical procedure described in our previous report.[17] Tetrahydrofuran was freshly distilled from sodium/benzophenone to ensure anhydrous conditions in the polymer synthesis (see the Supporting Information), and all other reagents were used without further purification.

2.2. Syntheses of PEEEET, PTOTT, and POT. Poly(3-{2-[2-(2-ethoxyethoxy)ethoxy]ethoxy}thiophene) (PEEEET) and poly(3-octylthiophene) (POT) were synthesized based on previously reported methods.[23,24] The synthesis of poly[3-(2,5,8,11-tetraoxatridecanyl)thiophene] (PTOTT) was performed using the Grignard metathesis (GRIM) polymerization method following a procedure similar to that used to synthesize POT and PTOTT (Scheme S1, Supporting Information).[25] Detailed synthetic procedures for PTOTT and complete characterization data are described in the Supporting Information. The chemical structures of the three polymers are presented in Figure 1A.

2.3. Oxidation of PEEEET. A small-scale oxidation of PEEEET was performed for the in situ measurements. In a typical experiment, 864, 932, and 966 μL of chloroform solutions each containing 5.15 nmol of PEEEET were mixed with 136, 68, and 34 μL of *m*-CPBA solution (13 mg/mL) in chloroform, respectively, to achieve the final *m*-CPBA concentrations of 2.5, 5, and 10 mM at the constant PEEEET concentration of 5.14 μM. The color of the solution gradually changed from deep blue to orange to yellow upon the addition of *m*-CPBA. The reaction progress was monitored by taking UV−vis absorption spectra and PL spectra at specific times after the addition of oxidant. Large-scale oxidation (approximately 10 times the small-scale amounts) and purification of oxidized samples were performed to quench the oxidation reaction and isolate the oxidized products for further IR characterization and QY measurements. A typical protocol for purification is as follows. When the desired emission color was obtained, the reaction was quenched with a saturated aqueous solution of sodium thiosulfate. A 10% (w/w) aqueous solution of sodium carbonate (Na_2CO_3) was then added into the two-phase mixture. The aqueous layer was removed, and the organic layer was washed with Na_2CO_3 solution three times and then with distilled water. The organic layer was isolated and dried over sodium sulfate, filtered into a clean vial, and evaporated to dryness. Absence of the oxidation byproduct, *meta*-chlorobenzoic acid, was confirmed by FTIR spectroscopy.

2.4. Characterization. IR spectra were obtained on a Perkin-Elmer system 2000 FTIR spectrometer. Electronic absorption spectra were acquired on an Agilent 8453 spectrophotometer. PL spectra were acquired on a Spex Fluorolog 3 equipped with a R928 PMT detector. QYs of oxidized PEEEET, pristine PTOTT, pristine POT, and pristine PEEEET were determined relative to known standards.[17] The standards used in the QY measurements were coumarin 102 (QY = 95% in ethanol, emission λ_{max} = 472 nm)[26] for oxidized PEEEET, coumarin 6 (QY = 78% in ethanol, emission λ_{max} = 505 nm)[27] for pristine POT and PTOTT, and cresyl violet (QY = 58% in ethanol, emission λ_{max} = 626 nm)[28] for pristine PEEEET. Each reported QY value was the average of at least three independent measurements.

2.5. Raman Measurements. Polymers were dissolved in chlorobenzene at a concentration of 5 mg/mL in a dry nitrogen environment. Thin films were spin-cast onto glass coverslips that were cleaned by sonicating in trichloroethylene, acetone, and methanol (15 min for each solvent) followed by UV-ozone treatment for 15 min.

Resonance Raman spectra of pristine PEEEET and POT thin films were recorded using a microscope-based spectrometer equipped with an Ar/Kr multicolor laser described in detail elsewhere.[29] To avoid photodegradation, all spectra were acquired in a wide-field geometry, and samples were placed in an inert gas flow cell. Excitation power densities were ∼1 KW/cm^2, and no sample degradation was observed over the spectral acquisition time (∼1−5 min).

2.6. Computational Methods. For each oligomer, an initial 3D structure was generated using Open Babel 2.3.1[30] (accessed through Pybel),[31] followed by a molecular mechanics minimization and stochastic Monte Carlo conformer search using the MMFF94 force field,[32−36] to find a low-energy minimum conformation. Final geometries were optimized using Gaussian 09[37] with density functional theory (DFT) B3LYP/6-31+G(d,p).[38,39] To match optical absorption spectra, time-dependent density functional theory (TDDFT) calculations were performed using the conductor polarizable continuum model (C-PCM) for CH_2Cl_2,[40,41] calculating the 10 lowest-energy excitations. In all cases, the lowest-energy optical excitation was used for excited-state geometry optimization to predict the fluorescence energy and oscillator strength.

3. RESULTS AND DISCUSSION

3.1. Optical Properties of Pristine PEEEET in Solution. PEEEET, a polythiophene with an alkoxy side chain, was

synthesized by the GRIM method reported by McCullough and co-workers.[24] Polythiophenes with two different side chains, POT and PTOTT (Figure 1), were also synthesized by the GRIM method (Supporting Information) for comparison. The regioregularity (>95% HT) of the polymers was confirmed by ^{1}H NMR spectroscopy. The molecular weights and polydispersities of the three polymers were determined by gel permeation chromatography (Table 1). Note that both POT and PTOTT have α-carbon atoms on their side chains, while PEEEET has an oxygen atom directly attached to the aromatic ring.

Table 1. Characterization of the Different Polythiophenes Used in the Study

polymer	$M_{n,GPC}$	M_w/M_n	λ_{max} (nm)	ε (M^{-1} cm^{-1})	λ_{em} (nm)	Φ_F (%)
pristine PEEEET	13 000	1.21	600	280 000	n.d.[a]	$\ll 1$[b]
PTOTT	12 148	1.18	440	160 000	565	17 ± 1.4
POT	11 480	1.13	450	89 000	575	14 ± 0.7
oxidized PEEEET	n.d.[a]	n.d.[a]	390	n.d.[a]	465	5 ± 0.9

[a]Not determined. [b]The QY was too low to be reliably determined.

Table 1 summarizes the photophysical properties of the three polymers. POT shows the characteristic orange color PL of poly(3-alkylthiophenes) with the emission wavelength maximum (λ_{max}) at 575 nm (Figure 1).[42] PTOTT shows similar spectral characteristics as POT with the absorption λ_{max} at 440 nm and the emission λ_{max} at 565 nm. The slight ~10 nm blue shift of the absorption and emission λ_{max} of PTOTT from those of POT is attributed to the slight twist in the polythiophene backbone due to the relatively bulky oligo(oxyethylene) side chains. On the other hand, the absorption λ_{max} for PEEEET peaks at 600 nm, which is red shifted about 160 nm from that of PTOTT. This substantial red shift is attributed to the coplanar conformation of the thiophene rings in poly(3-alkoxythiophenes) as well as the electron-donating nature of the side chain.[43,44] The QYs of regioregular POT and PTOTT were measured to be 14 and 17%, respectively, which are close to literature values.[45] On the contrary, PEEEET was almost nonemissive with very low quantum yield in its pristine state (Figure 1B,D), which is consistent with previous reports for monoalkoxy-substituted polythiophenes.[19−22]

3.2. Oxidation-Induced PL of PEEEET. To investigate the oxidation of PEEEET, a mild oxidant, *m*-CPBA, was added to a chloroform solution of PEEEET. Interestingly, the nonemissive solution of PEEEET started showing red fluorescence upon the addition of *m*-CPBA (Figure 2A,B). The PL intensity increased with the degree of oxidation over time, which was accompanied by the spectral blue shift (Figure 2B) and corresponding emission color changes from red to green (Figure 2A). The QY of oxidized PEEEET reached 5% when the emission maximum was 465 nm. Further oxidation eventually led to the reduction of PL intensity (Figure S1, Supporting Information). At any point of oxidation, the reaction can be quenched with sodium thiosulfate to obtain the desired PL colors (Figure 2A). When 7.2 μM PEEEET/chloroform solution was reacted with 5.2 mM *m*-CPBA in chloroform, red, orange, yellow, and green PL were typically observed after 1 min, 5 min, 1 h, and 2 h of oxidation, respectively.

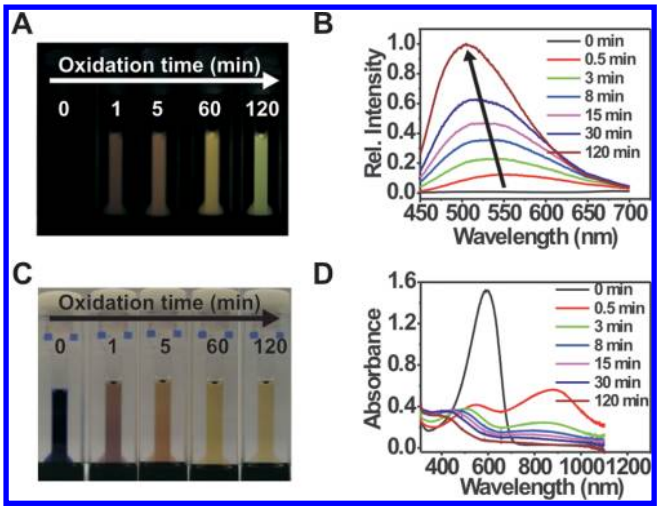

Figure 2. Photograph of PEEEET solutions (7.2 μM) in chloroform oxidized by 5.2 mM *m*-CPBA in chloroform at various times (A) under UV irradiation (λ_{exc} = 365 nm) and (C) under ambient light. (B) PL spectra and (D) absorption spectra of PEEEET solutions (5.14 μM) in chloroform oxidized with 10 mM *m*-CPBA in chloroform at different reaction times (λ_{exc} = 430 nm).

The color of the solution under room light also changed with oxidation from deep blue to yellow (Figure 2C). The in situ monitoring of the UV−vis absorbance showed an initial drop in the optical density of PEEEET along with the temporary appearance of a polaron band at ~900 nm, which is characteristic of doped poly(3-alkoxythiophenes)[44,46] (Figure 2D). Futher oxidation induced the blue shift of the $\pi-\pi^*$ transition in the absorption spectrum from 600 to ~400 nm as well as disappearance of the polaron peak (Figure 2D).

For comparison, the effects of oxidation on the optical properties of alkyl- and oligo(oxyethylene)-substituted polymer analogues, POT and PTOTT, were examined side by side, and their time-dependent PL characteristics are plotted in Figure 3A and B (see the Supporting Information for details). As expected,[11,47] POT showed efficient PL quenching upon the addition of *m*-CPBA. Although the degree of PL quenching is less severe in PTOTT than that in POT, PTOTT also showed the typical oxidation-induced PL quenching. Eventually, PEEEET became brigher than PTOTT and POT with prolonged oxidation. Time-dependent PL and absorption spectra of POT and PTOTT are presented in the Supporting Information (Figure S2).

The oxidation rate and the emission characteristics of PEEEET can be controlled by changing the concentration of oxidants as well as the reaction time (Figure 3); thus, the oxidation-induced fluorescence increase can potentially be used as an analytical tool for oxidants. Generally, sensing by PL increase is advantageous over the detection mechanisms based on PL quenching because most organic fluorophores are susceptible to photobleaching. Figure 3C presents the PL spectra of PEEEET with varying amounts of *m*-CPBA, and Figure 3D plots the time- and concentration-dependent PL response. A linear correlation between fluorescence intensity and the concentration of *m*-CPBA was obtained in the range of 13−70 μM, giving a detection limit of 9 μM using 5.14 μM PEEEET (Figure S3B, Supporting Information). To test if the oxidation-induced PL can be induced by other oxidants, hydrogen peroxide, another common oxidant, was also used to cause the oxidation of PEEEET (Figure S3C, Supporting

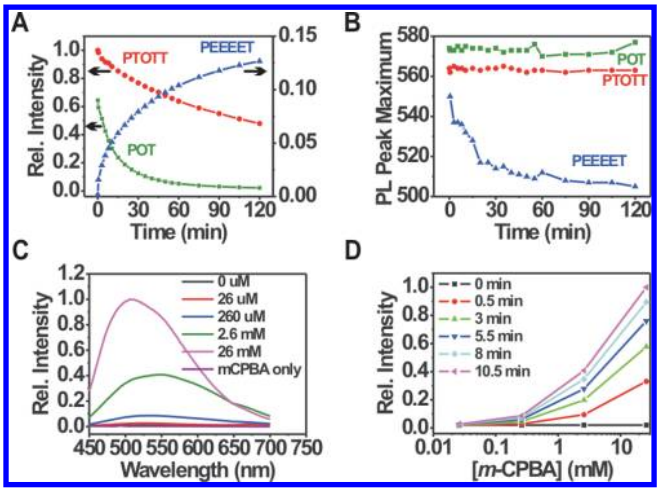

Figure 3. Rate of oxidation of PEEEET (5.14 μM) with *m*-CPBA (10 mM), followed by measuring the (A) PL intensity and (B) PL peak maximum as a function of reaction time. POT and PTOTT controls are shown as well. Because PEEEET is dark, the emission maximum of pristine PEEEET (at zero time) is not indicated. (C) PL spectra of PEEEET solutions (5.14 μM) in chloroform oxidized for 10.5 min at varying concentrations of *m*-CPBA. (D) Fluorescence response of 5.14 μM PEEEET in chloroform to various concentrations of *m*-CPBA at different oxidation times.

Information). An oxidation catalyst, methylrheniumtrioxide (MTO), was used to facilitate the reaction with hydrogen peroxide, which was previously reported to oxidize thiophene units to thiophene *S*-oxides and thiophene *S*,*S*-dioxides.[48] Similarly to the response to *m*-CPBA, PL started to significantly increase at micromolar concentrations (>10 μM) of hydrogen peroxide, showing that the oxidation-induced PL is not unique to *m*-CPBA (Figure S3C, Supporting Information).

3.3. Characterization of Oxidation Products. Poly(3-alkoxythiophenes) are known to be susceptible to oxidation and are stable in both neutral and oxidized states because of their low oxidation potentials.[23,44] Thiophene-*S*,*S*-dioxides are typical oxidation products of thiophenes and *m*-CPBA.[49,50] FTIR spectroscopy was used to identify the oxidation products of PEEEET (Figure 4). Table 2 presents FTIR peak assignments of oxidized PEEEET in comparison with pristine PEEEET. Strong absorption bands at ~1260 and ~1100 cm^{-1} of oxidized PEEEET were assigned to asymmetric and symmetric SO_2 stretches of sulfonyl groups.[13,51−53] Although the peaks at 1000−1100 cm^{-1} can be assigned to C−O stretching of the oligo(oxyethylene) substituents as well, the intensity in this region increased with oxidation, indicating that the S═O stretching contributes to the peak at 1000−1100 cm^{-1} in the oxidized PEEEET. Carbonyl compounds are also reported to be typical oxidative degradation products of polythiophenes.[13] In the oxidized PEEEET however, the carbonyl peak at 1700−1780 cm^{-1} is not as intense as the S═O peaks, indicating that thiophene-*S*,*S*-dioxides are the main reaction product for the oxidation of PEEEET.

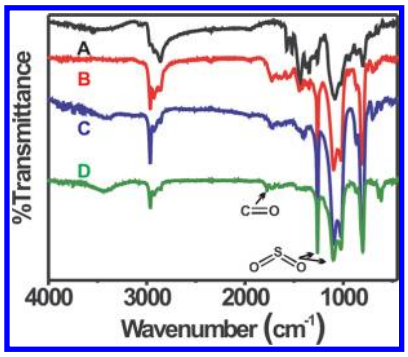

Figure 4. FTIR spectra of KBr pellets of (A) pristine PEEEET and oxidized PEEEET emitting (B) red, (C) orange, and (D) yellow light.

Table 2. Characteristic Infrared Absorptions of Pristine and Oxidized PEEEET

wavenumber (cm^{-1})		
pristine PEEEET	oxidized PEEEET	assignment[a]
2956	2962	CH_3 asymmetric stretch
2919	2923	CH_2 in-phase vibration, CH_2 asymmetric stretch
2850	2854	CH_2 out-of-phase vibration, CH_2 symmetric stretch
	1794, 1770, 1726, 1626	C═O stretch
1575, 1525		C═C asymmetric ring stretch
1440	1463	C═C symmetric ring stretch
1381	1378	CH_3 deformation
1260 (weak)		C−C inter-ring bond stretch
	1101, 1262 (strong)	symmetric and asymmetric SO_2 stretches
1080−1090	1106−1022	C−O−C stretching
802	801	out-of-plane C−H deformation

[a]From refs 11, 13, 51, and 52.

3.4. Characterization of Excited-State Structural Displacements of PEEEET. Resonance Raman spectra were measured to gain insights into the extent of π-conjugation and the excited-state geometrical displacements in PEEEET and POT thin films (Figure 5). It was not possible to obtain resonance Raman spectra for oxidized PEEEET due to broad and strong PL backgrounds that overwhelmed the signals. The

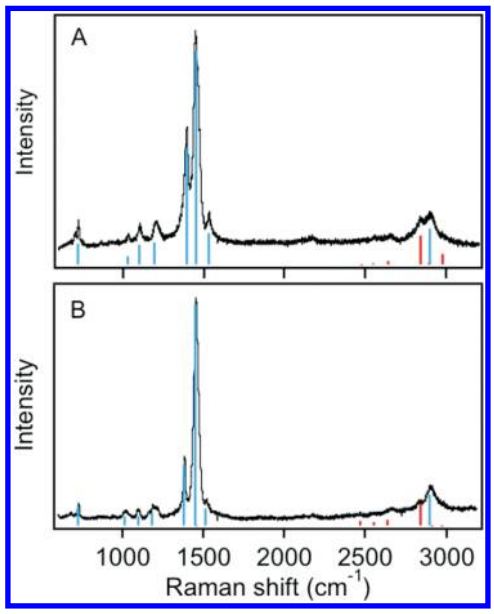

Figure 5. Comparison of calculated and experimental Raman spectra of (A) pristine PEEEET and (B) POT. Blue sticks represent fundamental and overtone intensities, and red sticks denote combination bands.

dominant peaks at ~1450 and ~1380−1390 cm^{-1} in the spectra are assigned to fundamental transitions of the C═C stretch (ν_6) and C−C symmetric stretch (ν_5), respectively. Frequencies for other backbone fundamental transitions are provided in Table 3. Note that PEEEET shows a substantially smaller relative intensity of the C═C mode (ν_6) to the intensity of the C−C mode (ν_5) than POT. In addition, the C−C stretching frequency of PEEEET blue shifts by about 10 cm^{-1} from that of POT, indicating significant charge transfer into C−C bonds from C═C bonds in PEEEET.[54] These results support increased planarity of PEEEET in the ground state, which is consistent with the smaller optical band gap.[55]

Table 3. Frequencies ($\hbar\omega_k$) and Fitted Mode-Specific, Dimensionless Vibrational Displacements (Δ_k) Used to Calculate Raman Spectra Including Overtone Combination Bands of PEEEET and POT[a]

	PEEEET		POT	
mode (k)	$\hbar\omega_k$ (cm^{-1})	Δ_k	$\hbar\omega_k$ (cm^{-1})	Δ_k
ν_1	723	0.86	728	0.34
ν_2	1029	0.40	1016	0.17
ν_3	1103	0.53	1098	0.16
ν_4	1198	0.51	1185	0.18
ν_5	1392	0.93	1383	0.31
ν_6	1450	1.20	1450	0.55
ν_7	1528	0.46	1517	0.14
E_{0-0} (cm^{-1})	13 500		16 722	
Γ (cm^{-1})	950		460	

[a]The excitation frequency (ω_I) was 20492 cm^{-1}.

Both PEEEET and POT spectra display distinct overtone and combination band transitions in addition to fundamental bands (Figure 5). PEEEET shows two resolved overtones in the C═C stretch at ~2900 cm^{-1} ($2\nu_6$) and ~4350 cm^{-1} ($3\nu_6$) accompanied by C═C/C−C combination bands (Figure 5 and Figure S4A, Supporting Information). The POT spectrum also shows one resolved overtone at ~2900 cm^{-1} ($2\nu_6$) as well as a C═C/C−C combination band (Figure 5). Analysis of the relative intensities of the fundamental bands and overtones can be used to probe structural displacements between the ground and excited states. We quantitatively analyzed the resonance Raman intensities of both PEEEET and POT to estimate mode-specific excited-state displacements. The detailed procedure for the analysis is described elsewhere.[56] Briefly, the time-dependent Schrodinger equation is analytically solved to generate Raman intensities using the framework of Heller and co-workers.[57] For the analysis of ν_6 bands, we only considered the ~1450 cm^{-1} component, which is reasonable as it is the dominant contributor to this line shape (see the Supporting Information). The key input parameter is the mode-specific vibrational displacement, Δ, which is adjusted until a good fit with experimental data is obtained. The procedure was simplified by using relative displacements determined from the Savin approximation, which relates these values to the relative intensities for each mode. The calculated Raman intensities are plotted in Figure 5 along with the experimental data, and the fitted displacements are summarized in Table 3 for each mode appearing in the Raman spectrum. Overall, the calculated intensities reproduced the experimental data well including the overtone region. The comparison of Δ between PEEEET and POT (Table 3) reveals larger values for PEEEET, most notably in the ν_6 mode, indicating that the PEEEET excited state undergoes larger geometry changes compared to POT. The large displacement should result in larger nonradiative rate constants,[58] contributing to the low QY of PEEEET.

3.5. Molecular Modeling and Mechanism for the Oxidation-Induced PL of PEEEET. To further understand the oxidation-induced fluorescence increase of PEEEET, we performed molecular modeling as described above. Electronic calculations on a pentamer of PEEEET showed that the insertion of one central thiophene-*S*,*S*-dioxide moiety red-shifted the optical absorption band gap from 2.18 to 1.74 eV and red-shifted the emission from 1.33 to 1.29 eV, consistent with previous reports on oligothiophenes and polythiophenes.[59,60] This result would directly contradict the experimentally observed blue shifts in PEEEET (Figure 2). Therefore, the oxidation-induced blue shift of PEEEET cannot be explained by the electronic effect of sulfonation alone. In addition, little changes were found in the PL oscillator strength of the monomeric analogues before and after oxidation (Table 4), indicating that again the oxidation-induced PL of PEEEET cannot be explained by the changes in the nature of the monomer unit.

Table 4. Calculated Photophysical Properties of Monomeric Analogues of Pristine and Oxidized PEEEET

	Absorption Energy (eV)[a]	Absorption Strength	Fluorescence Energy (eV)	Fluorescence Strength
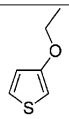	5.03 5.79	0.107 0.119	4.22	0.199
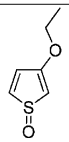	3.52 5.90	0.024 0.156	4.94	0.245
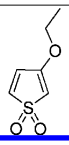	3.90 5.21	0.021 0.130	5.36	0.164

Rather, we attribute the oxidation-induced PL intensity increase of PEEEET to a conformational change and the reduction of conjugation length upon oxidation. A computational study indicated that alkoxythiophene dimers adopt a more planar conformation than alkylthiophene dimers due to increased delocalization induced by alkoxy side chains and intramolecular S···O interactions,[61] which was also suggested to be responsible for the planar structure of a technologically important polymer, poly(3,4-ethylenedioxythiophene) (PEDOT).[62] The significantly red-shifted absorption spectra of PEEEET relative to POT is consistent with the unusually planar conformation.

The thiophene-*S*,*S*-dioxide units introduced by oxidation can distort the initially planar conformation of pristine PEEEET and can lead to a higher energy gap and the corresponding blue shift in both absorption and PL spectra (Figure 2B, D). The oxidized PEEEET exhibits broad emission spectra whose peak positions change with excitation wavelengths (Figure S5, Supporting Information), indicating that there is a large

distribution of conjugation lengths in oxidized PEEEET. The shorter conjugation length and the large energy gap in oxidized PEEEET can lead to a reduced rate of nonradiative decay according to the energy gap law (see the Supporting Information),[58] converting nonemissive PEEEET to a light-emitting one (Figure 2). Although the thiophene-*S*,*S*-dioxide moieties can provide new channels for nonradiative decay,[45,63] the effect of conjugation length is apparently more dominant. A similar PL increase was reported for a poly(4-methyl-3-alkoxythiophene) (P4M3AOT),[46,64] where the steric effect provided by the methyl group in P4M3AOT induced a twisted conformation of the polymer backbone,[46] which reduced its conjugation length and caused a 10-fold increase in the PL.[64] This result is consistent with our oxidation-induced PL turn-on response.

The molecular modeling of a pentamer analogue of PEEEET showed that the introduction of an *S*,*S*-dioxide defect to pentaethoxyquinquethiophene distorts the standard conformation of pentaethoxyquinquethiophene, consistent with experimental data (Figure 6A). When the dihedral potential around the central inter-ring bond in a PEEEET pentamer is examined (Figure 6B), the defect forces a different dihedral angle and a significantly different torsional profile. Higher concentrations of *S*,*S*-dioxide defects lead to clear chain backbone twisting. For example, two neighboring *S*,*S*-dioxide rings lead to an optimized dihedral angle of 28.8° (Figure 6B). In addition, the defects interrupt the transoid alternation of side groups (Figure 6B, blue curve), which can disrupt the solid-state structure, because the side chains can no longer adopt the preferred interleaved comb-like motif.[65]

3.6. Solid-State Behavior. The conformational change of PEEEET upon oxidation can have important implications in the solid-state properties of the polymer. Figure 7A shows photographs of dried oxidized PEEEET in comparison to thin films of PEEEET, PTOTT, and POT. As expected, the thin film of POT was almost nonfluorescent due to the efficient packing of alkyl side chains.[65] PTOTT also showed efficient PL quenching in the solid state, showing only a dim fluorescence. On the other hand, as predicted by the molecular modeling (Figure 6), oxidized PEEEET shows bright PL in the solid state as well as in solution, presumably due to the bulky sulfonyl groups and disrupted side-chain packing, preventing close interaction of the polymer chains in the solid state. This result is consistent with previous work reporting that the oxidation of oligothiophene to oligothiophene-*S*,*S*-dioxides increased the solid-state PL quantum yield.[50,59] As the high PL of oxidized PEEEET is maintained in the solid state, the oxidant detection can be performed in the solid state as well as in solution. To test the solid-state behavior, a drop of PEEEET solution and a drop of the *m*-CPBA solution were sequentially placed on a thin-layer chromatography (TLC) plate (Figure 7B). The appearance of PL was readily observed in a few minutes (Figure 7B, bottom). The blue to yellow color change (Figure 7B, top) is also readily visible upon oxidation, providing an additional readout channel.

4. CONCLUSION

A poly(3-alkoxythiophene), PEEEET, showed unusual PL turn-on response upon the oxidation with *m*-CPBA. PEEEET showed a significantly red-shifted absorption spectrum compared to that of polyalkylthiophenes due to the electron-donating side chain and the planar conformation and is almost nonfluorescent in its pristine state. Resonance Raman measure-

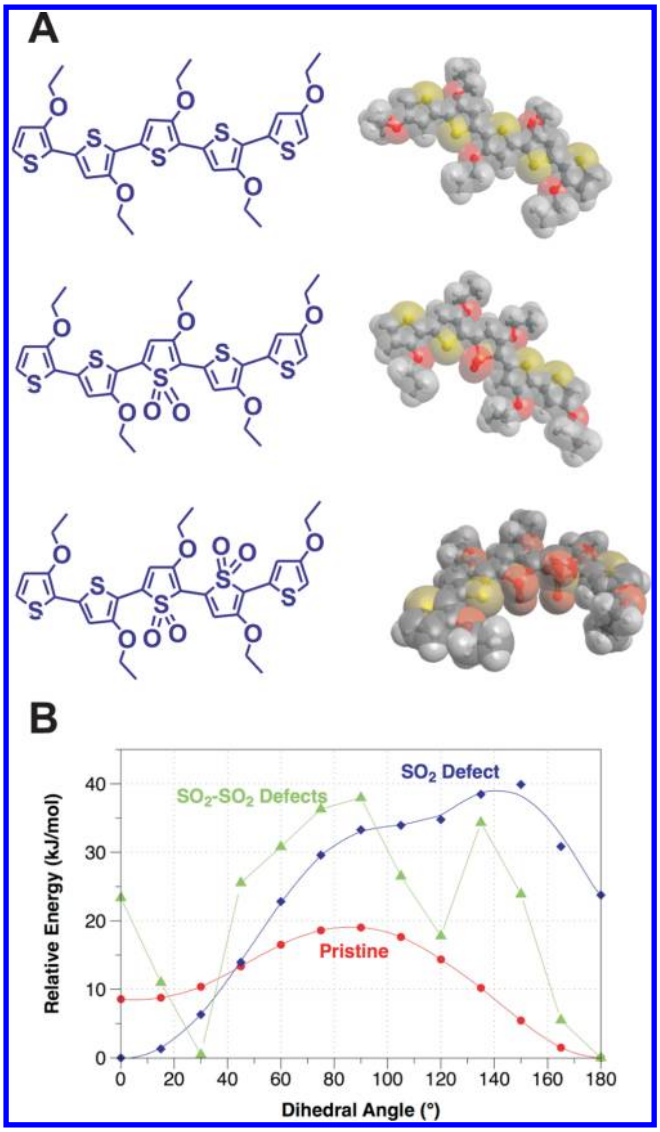

Figure 6. (A) Chemical structures and space-filling models of a pristine PEEEET pentamer (top), a PEEEET pentamer with one *S*,*S*-dioxide defect (middle), and a PEEEET pentamer with two *S*,*S*-dioxide defects (bottom). White, gray, yellow, and red colors represent hydrogen, carbon, sulfur, and oxygen atoms, respectively. (B) Corresponding B3LYP-computed relative energies for dihedral rotation around the central inter-ring bond for the structures in (A). Note that the SO_2 defect dramatically increases the torsional barrier and forces a different conformation, where alkoxy side chains adopt a cis rather than trans conformation.

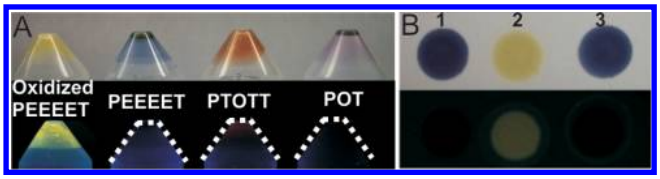

Figure 7. (A) Photographs of films of oxidized PEEEET, pristine PEEEET, PTOTT, and POT dried from chloroform solution in polypropylene tubes under ambient light (top) and under illumination at 365 nm (bottom). (B) Drop-cast films from PEEEET in chloroform on a TLC plate before (1) and after (2) oxidation with *m*-CPBA in ethyl acetate under ambient light (top) and under illumination at 365 nm (bottom). Also shown is a control with only ethyl acetate added to PEEEET film (3).

ments on PEEEET and POT thin films were consistent with the unusually coplanar conformation of PEEEET. The Raman data also showed that PEEEET undergoes larger structural displacements between the ground and excited states compared to POT, consistent with the very low emission QY of PEEEET. Upon the addition of *m*-CPBA, bright fluorescence was observed from the PEEEET solution with increasing PL intensity with time and the amount of oxidants. The PL increase was accompanied by blue shifts in the absoption and emission spectra. The IR measurements of oxidized species indicated that thiophene-*S*,*S*-dioxide is the main oxidation product. The molecular modeling on oligomeric analogues showed that the bulky thiophene-*S*,*S*-dioxide moieties distort the planar conformation and the transoid alternation of side chains, which is consistent with the bright PL of oxidized PEEEET in the solid state as well as in solution. The molecular modeling also showed that the introduction of thiophene-*S*,*S*-dioxide defects to oligomeric analogues induced red shifts in absorption and emission spectra and did not cause large changes in oscillator strengths of monomers. This result indicates that the oxidation-induced PL increase cannot be explained by the nature of monomers and changes in radiative rates. Therefore, we attribute the unusual oxidation-induced fluorescence increase of PEEEET to the distorted conformation and the reduced conjugation lengths, which decrease the probability of nonradiative decay in accordance with the energy gap law.[58]

■ ASSOCIATED CONTENT

Ⓢ Supporting Information

Detailed syntheses and characterization of PEEEET, POT, and PTOTT, additional PL spectra of oxidation of PEEEET, absorption and PL spectra of oxidation of POT and PTOTT, PL spectra at micromolar concentrations of *m*-CPBA for measurement of the detection limit, PL spectra of oxidation of PEEEET with H_2O_2/MTO, resonance Raman spectra of PEEEET and POT at different excitation wavelengths, PL spectra of PEEEET at different excitation wavelengths, solution and film absorption spectra of PEEEET and poly(3-hexylthiophene) (PHT), calculated absorption and emission data on PEEEET oligomers, and estimation of the changes in the nonradiative rate and the radiative rate upon the oxidation of PEEEET with sample data. This material is available free of charge via the Internet at http://pubs.acs.org.

■ AUTHOR INFORMATION

Corresponding Author

*E-mail: sojungp@sas.upenn.edu (S.J.P.). Contact jkgrey@unm.edu (J.K.G.) for Raman studies. Contact geoffh@pitt.edu (G.R.H.) for computational studies.

Author Contributions

⊥These authors contributed equally.

Notes

The authors declare no competing financial interest.

The manuscript was written through contributions of all authors. All authors have given approval to the final version of the manuscript.

■ ACKNOWLEDGMENTS

S.J.P. acknowledges support from the Penn Nano/Bio Interface Center (NSF DMRO8-32802) and the ARO young investigator award (W911Nf-09-1-014). A.C.K. acknowledges support from the Nano/Bio Interface Center through the National Science Foundation IGERT DGE02-21664.

■ REFERENCES

(1) Grimsdale, A. C.; Leok Chan, K.; Martin, R. E.; Jokisz, P. G.; Holmes, A. B. *Chem. Rev.* **2009**, *109*, 897−1091.
(2) Facchetti, A. *Chem. Mater.* **2011**, *23*, 733−758.
(3) Thomas, S. W.; Joly, G. D.; Swager, T. M. *Chem. Rev.* **2007**, *107*, 1339−1386.
(4) Feng, X.; Liu, L.; Wang, S.; Zhu, D. *Chem. Soc. Rev.* **2010**, *39*, 2411−2419.
(5) Kim, H. N.; Guo, Z.; Zhu, W.; Yoon, J.; Tian, H. *Chem. Soc. Rev.* **2011**, *40*, 79−93.
(6) Tian, Z.; Yu, J.; Wu, C.; Szymanski, C.; McNeill, J. *Nanoscale* **2010**, *2*, 1999−2011.
(7) Pecher, J.; Mecking, S. *Chem. Rev.* **2010**, *110*, 6260−6279.
(8) Duarte, A.; Pu, K.-Y.; Liu, B.; Bazan, G. C. *Chem. Mater.* **2011**, *23*, 501−515.
(9) Cumpston, B. H.; Parker, I. D.; Jensen, K. F. *J. Appl. Phys.* **1997**, *81*, 3716−3720.
(10) Park, S.-J.; Gesquiere, A. J.; Yu, J.; Barbara, P. F. *J. Am. Chem. Soc.* **2004**, *126*, 4116−4117.
(11) Abdou, M. S. A.; Holdcroft, S. *Macromolecules* **1993**, *26*, 2954−2962.
(12) Koch, M.; Nicolaescu, R.; Kamat, P. V. *J. Phys. Chem. C* **2009**, *113*, 11507−11513.
(13) Manceau, M.; Rivaton, A.; Gardette, J.-L.; Guillerez, S.; Lemaître, N. *Polym. Degrad. Stab.* **2009**, *94*, 898−907.
(14) Hintz, H.; Egelhaaf, H. J.; Luer, L.; Hauch, J.; Peisert, H.; Chasse, T. *Chem. Mater.* **2011**, *23*, 145−154.
(15) Scurlock, R. D.; Wang, B.; Ogilby, P. R.; Sheats, J. R.; Clough, R. L. *J. Am. Chem. Soc.* **1995**, *117*, 10194−10202.
(16) Wu, C.; Bull, B.; Szymanski, C.; Christensen, K.; McNeill, J. *ACS Nano* **2008**, *2*, 2415−2423.
(17) Duncan, T. V.; Park, S.-J. *J. Phys. Chem. B* **2009**, *113*, 13216−13221.
(18) Dane, E. L.; King, S. B.; Swager, T. M. *J. Am. Chem. Soc.* **2010**, *132*, 7758−7768.
(19) Vangheluwe, M.; Verbiest, T.; Koeckelberghs, G. *Macromolecules* **2008**, *41*, 1041−1044.
(20) Zhang, Z.-B.; Fujiki, M. *Polym. J.* **2001**, *33*, 597−601.
(21) He, J.; Su, Z.; Yan, B.; Xiang, L.; Wang, Y. *J. Macromol. Sci., Part A* **2007**, *44*, 989−993.
(22) Van den Bergh, K.; Cosemans, I.; Verbiest, T.; Koeckelberghs, G. *Macromolecules* **2010**, *43*, 3794−3800.
(23) Sheina, E. E.; Khersonsky, S. M.; Jones, E. G.; McCullough, R. D. *Chem. Mater.* **2005**, *17*, 3317−3319.
(24) Jeffries-El, M.; Sauve, G. v.; McCullough, R. D. *Macromolecules* **2005**, *38*, 10346−10352.
(25) Loewe, R. S.; Ewbank, P. C.; Liu, J.; Zhai, L.; McCullough, R. D. *Macromolecules* **2001**, *34*, 4324−4333.
(26) Jones, G.; Rahman, M. A. *J. Phys. Chem.* **1994**, *98*, 13028−13037.
(27) Reynolds, G. A.; Drexhage, K. H. *Opt. Commun.* **1975**, *13*, 222−225.
(28) Rurack, K.; Spieles, M. *Anal. Chem.* **2011**, *83*, 1232−1242.
(29) Gao, Y.; Grey, J. K. *J. Am. Chem. Soc.* **2009**, *131*, 9654−9662.
(30) O'Boyle, N. M.; Banck, M.; James, C. A.; Morley, C.; Vandermeersch, T.; Hutchison, G. R. *J. Cheminformatics* **2011**, *3*, 33.
(31) O'Boyle, N. M.; Morley, C.; Hutchison, G. R. *Chem. Cent. J.* **2008**, *2*, 5.
(32) Halgren, T. *J. Comput. Chem.* **1996**, *17*, 490−519.
(33) Halgren, T. *J. Comput. Chem.* **1996**, *17*, 520−552.
(34) Halgren, T. *J. Comput. Chem.* **1996**, *17*, 553−586.
(35) Halgren, T.; Nachbar, R. *J. Comput. Chem.* **1996**, *17*, 587−615.
(36) Halgren, T. *J. Comput. Chem.* **1996**, *17*, 616−641.
(37) Frisch, M. J.; Trucks, G. W.; Schlegel, H. B.; Scuseria, G. E.; Robb, M. A.; Cheeseman, J. R.; Scalmani, G.; Barone, V.; Mennucci,

B.; Petersson, G. A.; et al. *Gaussian 09*, revision A.2; Gaussian, Inc.: Wallingford, CT, 2009.
(38) Becke, A. *J. Chem. Phys.* **1993**, *98*, 5648−5652.
(39) Lee, C.; Yang, W.; Parr, R. *Phys. Rev. B* **1988**, *37*, 785−789.
(40) Tomasi, J. *Theor. Chem. Acc.* **2004**, *112*, 184−203.
(41) Tomasi, J.; Mennucci, B. *Chem. Rev.* **2005**, *105*, 2999−3094.
(42) Chen, T.-A.; Wu, X.; Rieke, R. D. *J. Am. Chem. Soc.* **1995**, *117*, 233−244.
(43) Daoust, G.; Leclerc, M. *Macromolecules* **1991**, *24*, 455−459.
(44) Koeckelberghs, G.; Vangheluwe, M.; Samyn, C.; Persoons, A.; Verbiest, T. *Macromolecules* **2005**, *38*, 5554−5559.
(45) Xu, B.; Holdcroft, S. *Macromolecules* **1993**, *26*, 4457−4460.
(46) Chayer, M.; Faïd, K.; Leclerc, M. *Chem. Mater.* **1997**, *9*, 2902−2905.
(47) Holdcroft, S. *Macromolecules* **1991**, *24*, 4834−4838.
(48) Brown, K. N.; Espenson, J. H. *Inorg. Chem.* **1996**, *35*, 7211−7216.
(49) van Tilborg, W. J. M. *Synth. Commun.* **1976**, *6*, 583−589.
(50) Barbarella, G.; Pudova, O.; Arbizzani, C.; Mastragostino, M.; Bongini, A. *J. Org. Chem.* **1998**, *63*, 1742−1745.
(51) Yamamoto, T.; Nurulla, I.; Hayashi, H.; Koinuma, H. *Synth. Met.* **1999**, *107*, 137−141.
(52) Barbarella, G.; Favaretto, L.; Sotgiu, G.; Zambianchi, M.; Bongini, A.; Arbizzani, C.; Mastragostino, M.; Anni, M.; Gigli, G.; Cingolani, R. *J. Am. Chem. Soc.* **2000**, *122*, 11971−11978.
(53) Manceau, M.; Gaume, J.; Rivaton, A.; Gardette, J.-L.; Monier, G.; Bideux, L. *Thin Solid Films* **2010**, *518*, 7113−7118.
(54) Louarn, G.; Trznadel, M.; Buisson, J. P.; Laska, J.; Pron, A.; Lapkowski, M.; Lefrant, S. *J. Phys. Chem.* **1996**, *100*, 12532−12539.
(55) Dkhissi, A.; Louwet, F.; Groenendaal, L.; Beljonne, D.; Lazzaroni, R.; Brédas, J. L. *Chem. Phys. Lett.* **2002**, *359*, 466−472.
(56) Wise, A. J.; Grey, J. K. *Phys. Chem. Chem. Phys.* **2012**, *14*, 11273−11276.
(57) Heller, E. J.; Sundberg, R.; Tannor, D. *J. Phys. Chem.* **1982**, *86*, 1822−1833.
(58) Englman, R.; Jortner, J. *Mol. Phys.* **1970**, *18*, 145−164.
(59) Barbarella, G.; Favaretto, L.; Sotgiu, G.; Zambianchi, M.; Fattori, V.; Cocchi, M.; Cacialli, F.; Gigli, G.; Cingolani, R. *Adv. Mater.* **1999**, *11*, 1375−1379.
(60) Amir, E.; Sivanandan, K.; Cochran, J. E.; Cowart, J. J.; Ku, S.-Y.; Seo, J. H.; Chabinyc, M. L.; Hawker, C. J. *J. Polym. Sci., Part A: Polym. Chem.* **2011**, *49*, 1933−1941.
(61) Garcia, G.; Garzon, A.; Granadino-Roldan, J. M.; Moral, M.; Fernandez-Liencres, M. P.; Navarro, A.; Fernandez-Gomez, M. *Aust. J. Chem.* **2010**, *63*, 1297−1306.
(62) Poater, J.; Casanovas, J.; Solà, M.; Alemán, C. *J. Phys. Chem. A* **2009**, *114*, 1023−1028.
(63) Melo, J. S. d.; Burrows, H. D.; Svensson, M.; Andersson, M. R.; Monkman, A. P. *J. Chem. Phys.* **2003**, *118*, 1550−1556.
(64) Lévesque, I.; Leclerc, M. *Chem. Mater.* **1996**, *8*, 2843−2849.
(65) Mena-Osteritz, E.; Meyer, A.; Langeveld-Voss, B. M. W.; Janssen, R. A. J.; Meijer, E. W.; Bäuerle, P. *Angew. Chem., Int. Ed.* **2000**, *39*, 2679−2684.